# HYBRID VIBRATION EXPERIMENT ON SEISMIC BEHAVIOR OF A HIGHWAY BRIDGE ON LIQUEFIABLE GROUND

Keiichi Tamura[1], Mitsu Okamura[2] and Shunsuke Tanimoto[3]

## Abstract

In order to improve seismic design technology of highway bridges, it is most essential to investigate seismic behavior of a whole bridge system. For this purpose, we have developed a hybrid experiment technique, which integrates numerical response analysis with vibration experiment, and applied it for studying seismic behavior of highway bridge system including surrounding soils. In the present study we assumed a highway bridge on liquefiable ground, performed a series of hybrid vibration experiments, and examined the interactive seismic response of bridge pier and pile foundation and the influence of liquefaction on the dynamic response of highway bridge system.

## Introduction

In the seismic design of highway bridges, we generally divide a bridge into two parts, i.e., superstructure-pier and foundation. This is mostly for simplicity, however, there exists interaction between them, and studying this interaction is most essential to solve the seismic behavior of whole bridge system, which would contribute to the further development of seismic design technology. Vigorous efforts have been devoted to study this interaction analytically. On the other hand, experimental studies have been rather limited, because they generally require large-scale experiments.

Following the previous studies with a highway bridge on non-liquefiable ground (Kobayashi *et al.*, 2002, Tamura *et al.*, 2004), we examined in this study the seismic behavior of highway bridge system on liquefiable ground by using hybrid vibration experiment technique, which integrates numerical response analysis with vibration experiment. Based on the experimental results, we investigated the interaction between seismic response of bridge pier and foundation and the influence of liquefaction on the dynamic response of highway bridge system.

[1] Research Coordinator for Earthquake Disaster Prevention, National Institute for Land and Infrastructure Management, Tsukuba-shi, Ibaraki-ken Japan

[2] Associate Professor, Department of Civil and Environmental Engineering, Ehime University, Matsuyama-shi, Ehime-ken Japan

[3] Ground Vibration Research Team, Public Works Research Institute, Tsukuba-shi, Ibaraki-ken Japan

## Overview of Hybrid Vibration Experiment

As illustrated in Figure 1, an original structure is divided into two parts in the hybrid vibration experiment. One is an actual model specimen of original structure. This specimen is usually taken as a part of structure whose seismic behavior is unknown or complicated. The other is a numerical model for vibration response analysis. This model represents a part of structure whose seismic behavior can be evaluated by numerical analysis.

In our hybrid vibration experiment, we made a pile foundation and surrounding soils as the actual model, and footing, pier and girder as the numerical model. An outline of experimental process is as follows:

(1) Place a spacer and balance weight on the pile foundation model, and connect an actuator with the balance weight. For the vertical direction, adjust the weight of balance weight so that the total weight of spacer and balance weight corresponds to the dead weight of superstructure, pier and footing that acts on the pile foundation.
(2) Shake the table horizontally with an input motion, and measure the reaction force of model specimen at the boundary of specimen and numerical model. Compute response displacement of numerical model to this reaction force and external force such as inertia force.
(3) Apply the calculated displacement of numerical model to the specimen by the actuator and thus reproduce seismic response of highway bridge system. Note that we ignore the rotational motion in this experiment.

## Prototype and Experimental Model

The prototype of experimental model is a 30m-span simple girder bridge on the medium soil ground, which is schematically illustrated in Figure 2. This bridge was designed after the 1996 Design Specifications for Highway Bridges (Japan Road Association, 1996). To secure the consistency with our previous experiments with a highway bridge on non-liquefiable ground, we assumed in the present study the same bridge structure including a foundation with the highway bridge employed in the previous study.

The prototype bridge was reduced to 25% in size to produce an experimental model. Two piles in the longitudinal direction were extracted for the test specimen as shown in Figure 3. According to the number of piles of experimental model, we reduced the external force generated at the boundary of real specimen and numerical model to 25% of the prototype. Since the preliminary objective of this study is to examine nonlinear seismic response of both bridge pier and foundation, we used RC piles for experiments.

The number and diameter of reinforcing bars of a model pile were determined to be consistent with the reinforcement ratio of the prototype pile. The diameter and length of

model pile are 300mm and 3.0m, respectively. The pile heads were rigidly connected to the footing, while their tips were connected to the bottom of laminar shear box by hinges to allow rotation.

We employed two ground models in this study, i.e., one-layer liquefiable ground and liquefiable ground overlaid by the surface non-liquefiable layer. The former ground model is of 3m thick saturated silica sand. We constructed liquefiable and non-liquefiable grounds by adjusting the relative density of soils as 40% and 88%, respectively. The liquefiable loose ground was produced by boiling the sands. The non-liquefiable ground was built so that the relative density of soils was to be the target value by shaking the loose ground model on the shake table. The ground model with surface non-liquefiable layer was constructed by lowering the ground water level once after building liquefiable ground. The surface non-liquefiable layer was 1m thick.

## Vibration Response Analysis

The numerical model consists of structural elements (mass, damping and stiffness matrices), external force that is calculated from the acceleration of shaking table, and reaction force generated at the boundary of the actual and numerical models. In the numerical analysis, the external and reaction forces are inputted, and the displacement of actual model for the next time step is calculated. This displacement is realized by an actuator. Then, the external and reaction forces are measured and taken into numerical analysis. Iterating these procedures, the seismic behavior of original structure can be accurately simulated. The equation of motion for numerical analysis may be described as

$$M\ddot{x} + C\dot{x} + Kx = p + q \tag{1}$$

where

$M$: Mass matrix
$C$: Damping matrix
$K$: Stiffness matrix
$x$: Relative displacement vector
$p$: External force (seismic response) vector
$q$: Reaction force vector.

Using Eq. (1), the vibration response (displacement vector $x$) after a short interval $\Delta t$ can be calculated from the measured reaction force vector $q$ and the external force vector $p$. The central difference method is employed in vibration response analysis, because it requires short time to generate actuator signal for the next time step after measuring reaction force. Time required for one cycle process is 2.08ms (Umekita *et al.*, 1997).

As the numerical model, we assume a 2-degree-of-freedom system consisting of

mass of footing, and that of pier and girder. Figure 4 shows the force and displacement relationship of pier, which is idealized as a bi-linear system.

## Experimental Method

Although actuator response delay has unfavorable influence on the hybrid vibration experiment, it is inevitable with a hydraulic actuator. Consequently, a compensation technique is adopted. This technique predicts the displacement of an actuator at the time after actuator delay time (Horiuchi *et al.*, 1996).

As the input motions for experiments, we used sinusoidal waves with a frequency corresponding to the second natural frequency of bridge system, for which the vibration of bridge pier and superstructure is predominant. The reason we employed sinusoidal waves is because the experiment was our first hybrid vibration experiment with liquefiable soils and we intended to securely generate liquefaction.

By utilizing the advantage of hybrid vibration experiment, we variously changed the property of bridge pier. We assumed both linear and bi-linear systems for the bridge pier. In addition to this, we also assumed the retrofitted bridge pier, for which both the initial rigidity and yield displacement were set as 1.2 times of the original bridge pier. To secure stability of the hybrid vibration experiment, we expanded the time axis of input motions three times as long as the original time axis. Table 1 summarizes the experimental cases.

## Experimental Results

### Influence of liquefaction

Figure 5 shows the time histories of excess pore water pressure ratio, which were observed 0.95m beneath the spacer. The excess pore water pressure ratio is generally less than 0.5 for Case C3, in which the relative density of the ground was adjusted as 88%. This fact signifies that the ground did not liquefy in this case. While it reached 1.0 after a few cycles from the beginning and maintained this level during the excitation for Case C4, in which the relative density was 40%.

Figure 6 plots the acceleration time histories recorded 0.95m beneath the spacer for Cases C3 and C4. Accelerations on the shake table, which are the input motions of experiments, are also plotted in this figure. In Case C3 the ground acceleration 0.95m beneath the surface is almost similar to the input motion. By contrast, the ground acceleration in Case C4 decreases quickly after a few cycles from the beginning. This is harmonic with the change of excess pore water pressure ratio presented in Figure 5.

Figure 7 compares the shear force at pile head, accelerations at footing and superstructure for Cases C3 and C4. Note that the bridge pier is assumed to be elastic and

the input motion is sinusoidal wave with frequency corresponding to the second natural frequency of the bridge system in both cases. The shear force at pile head, accelerations at footing and superstructure are almost identical between those two cases at the beginning of experiment when the ground did not liquefy. While after the ground liquefied, the shear force and accelerations in Case C4 become smaller than those in Case C3. This may be attributed to the fact that the ground acceleration decreases in Case C4 as indicated in Figure 6 and the seismic response of bridge pier and superstructure becomes small. The frequency of input motion coincides with the second natural frequency of the bridge system, and the vibration of bridge pier and superstructure is predominant in this second vibration mode.

Influence of plasticity generated in bridge pier

Figure 8 shows the relationships between horizontal force and displacement of bridge pier for Cases C3 and C5. Note that the relative density of ground is 88% in both cases and the ground did not liquefy. The bridge pier in Case C3 remained elastic, whereas the pier in C5 became plastic. Figure 9 plots time histories of shear force at pile head, accelerations at footing and superstructure for those two cases. Results are identical for the first several cycles of excitation before the pier became plastic. After that, the response amplitudes in Case C5 become smaller than those in C3 in general. The change of period in structural response is unclear within the scope of present study. Figure 10 shows pile curvatures at pile head, intermediate part and pile tip for Cases C3 and C5. Similar to Figure 9, the pile curvatures in C5 become smaller than those in C3 after the pier behaves plastically. This is most significant at the pile head.

The above results are for non-liquefiable ground, while the results for liquefiable ground, i.e., Cases C4 and C6, are presented below. We assumed an elastic pier and plastic pier in C4 and C6, respectively. The lateral force and displacement relationships of bridge pier are plotted in Figure 11 for C4 and C6. Figure 12 shows the shear force at pile head, accelerations at footing and superstructure for those two cases. The difference between C4 and C6 is less significant as compared to the difference between C3 and C5. This may be attributed to a fact that the degree of plasticity is smaller in C6 than in C4. The pile curvatures are plotted for the three different locations in Figure 13.

Influence of surface non-liquefiable layer

Similar to Figure 5, time histories of the excess pore water pressure ratio monitored 1.35m beneath the spacer in Cases C12 and C15 are plotted in Figure 14. Note that C12 has the surface non-liquefiable layer and C15 does not have one. As seen from Figure 14, the excess pore water pressure rose slowly in Case C12, comparing to C15.

Acceleration response time histories are shown in Figure 15. The ground acceleration followed the shake table acceleration immediately after the beginning of excitation, and then reached the almost constant amplitude due to the occurrence of liquefaction.

The lateral force and displacement relationships of bridge pier are shown in Figure 16 for Cases C12 and C15. Figure 17 compares the shear force at pile head, accelerations at footing and superstructure for those two cases. From Figure 17 we cannot find significant difference in structural response between those two cases. This may be due to a fact that the footing is located on the ground surface in both cases, and the existence of surface non-liquefiable layer did not affect much the seismic response of structure.

## Conclusions

We have developed a hybrid vibration experiment technique, and applied it for studying seismic behavior of a highway bridge on liquefiable ground. We conducted a series of hybrid vibration experiments, and investigated the interaction between seismic response of bridge pier and foundation and the influence of liquefaction on the dynamic response of highway bridge system. Main conclusions of the present study may be summarized as follows:

(1) The occurrence of liquefaction decreased the seismic response of both foundation and superstructure within the scope of the present study. This may be attributed to a fact that the input motion employed develops the second natural vibration mode, in which the vibration of bridge pier and superstructure is predominant, the seismic response of bridge pier and superstructure decreases after the ground liquefies, and this contributes to reduce dynamic response of the whole bridge system.
(2) The generation of plasticity in bridge pier also decreased the seismic response of both foundation and superstructure in the present study. This fact may be understandable with the input motions employed for experiments.
(3) The existence of surface non-liquefiable layer affected the accumulation of excess pore water pressure, though the location of structural members may have more dominant influence over the seismic response of a highway bridge.

## References


1) Horiuchi, T., Nakagawa, M., Sugano, M. and Konno, T.: Development of a Real-Time Hybrid Experimental System with Actuator Delay Compensation, *Proc. 11th World Conference on Earthquake Engineering*, 1996.
2) Japan Road Association: *Design Specifications for Highway Bridges, Part V, Seismic Design*, 1996 (in Japanese).
3) Kobayashi, H., Tamura, K. and Tanimoto, S.: Hybrid Vibration Experiments with a Bridge Foundation System Model, *Soil Dynamics and Earthquake Engineering*, Vol.22, No.9-12, 2002.
4) Tamura, K., Kobayashi, H., Tanimoto, S. and Okamura, M.: Hybrid Vibration Experiment on Interactive Response of Superstructure and Foundation of Highway

Bridge, *Proc. 13th World Conference on Earthquake Engineering*, 2004.
5) Umekita, K. *et al.*: Development of C Language Library for Super Real-Time Controller (SRC) for Real-Time Hybrid Seismic Testing System with Three-dimensional-in-plane Excitation, *Proc. 40th Japan Joint Automatic Control Conference*, 1997 (in Japanese).

Table 1 Experimental cases

(a) Cases without surface non-liquefiable layer

| Case No. | Input motion | | Bridge pier | Relative density | Natural frequency | | Ground model |
|---|---|---|---|---|---|---|---|
| | Peak accel. | Frequency | | | 1st mode | 2nd mode | |
| C3 | 0.6G | 36 Hz | Elastic | 88% | 9.99 Hz | 36.9 Hz | Non-liquefiable |
| C4 | 0.6G | 36 Hz | Elastic | 40% | 7.53 Hz | 35.6 Hz | Initial |
| | | | | | 3.57 Hz | 34.6 Hz | Liquefied |
| C5 | 0.6G | 36 Hz | Bi-linear | 88% | 9.99 Hz | 36.9 Hz | Non-liquefiable |
| C6 | 0.6G | 36 Hz | Bi-linear | 40% | 7.53 Hz | 35.6 Hz | Initial |
| | | | | | 3.57 Hz | 34.6 Hz | Liquefied |
| C8 | 0.6G | 39 Hz | Retrofitted Bi-linear | 40% | 7.59 Hz | 38.8 Hz | Initial |
| | | | | | 3.57 Hz | 37.8 Hz | Liquefied |

(b) Cases with surface non-liquefiable layer

| Case No. | Input motion | | Bridge pier | Relative density | Water level | Natural frequency | | Ground model |
|---|---|---|---|---|---|---|---|---|
| | Peak acc | Freq | | | | 1st mode | 2nd mode | |
| C12 | 1.1G | 39 Hz | Bi-linear | 40% | -1m | 7.53 Hz | 35.6 Hz | Initial |
| | | | | | | 4.02 Hz | 34.6 Hz | Liquefied |
| C13 | 1.1G | 36 Hz | Elastic | 40% | -1m | 7.53 Hz | 35.6 Hz | Initial |
| | | | | | | 4.02 Hz | 34.6 Hz | Liquefied |
| C14 | 1.1G | 39 Hz | Retrofitted Bi-linear | 40% | -1m | 7.53 Hz | 35.6 Hz | Initial |
| | | | | | | 4.02 Hz | 34.6 Hz | Liquefied |
| C15 | 1.1G | 36 Hz | Bi-linear | 40% | 0m | 7.53 Hz | 35.6 Hz | Initial |
| | | | | | | 3.57 Hz | 34.6 Hz | Liquefied |
| C16 | 1.1G | 39 Hz | Elastic | 40% | 0m | 7.53 Hz | 35.6 Hz | Initial |
| | | | | | | 3.57 Hz | 34.6 Hz | Liquefied |
| C17 | 1.1G | 36 Hz | Retrofitted Bi-linear | 40% | 0m | 7.53 Hz | 35.6 Hz | Initial |
| | | | | | | 3.57 Hz | 34.6 Hz | Liquefied |

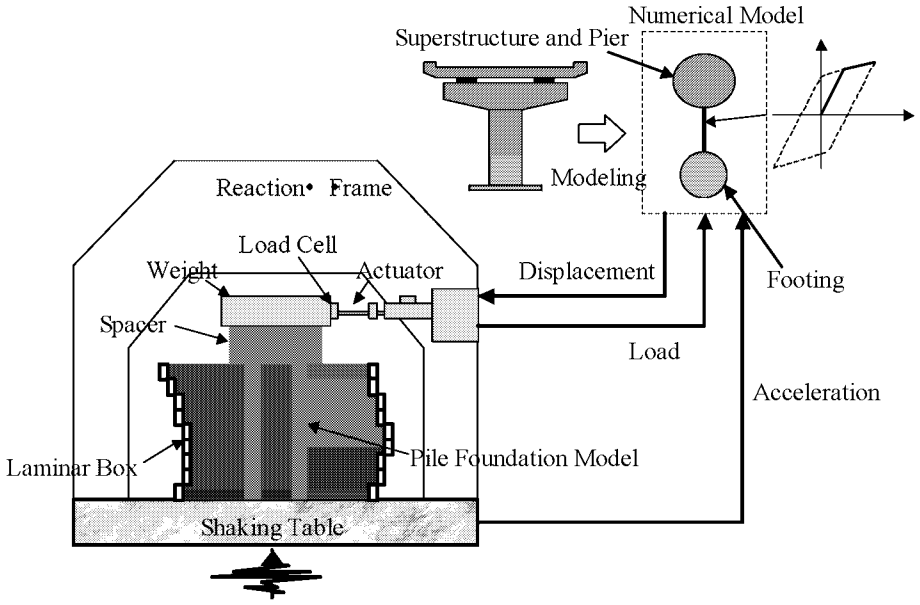


Figure 1 Conceptual view of hybrid vibration experiment

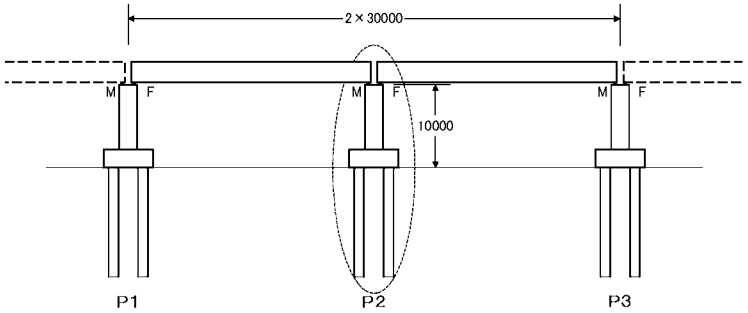


Figure 2 Schematic view of prototype bridge

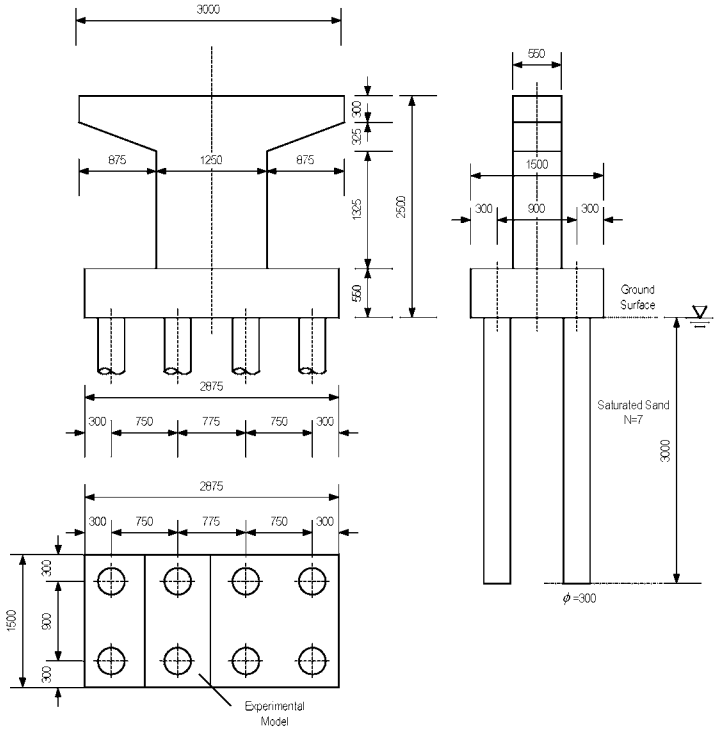


Figure 3 Overview of experimental model

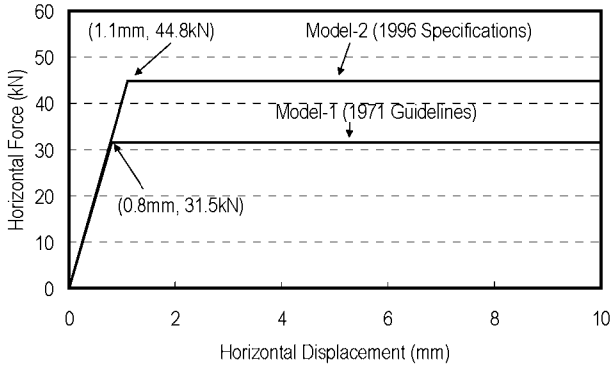


Figure 4 Horizontal force-displacement relationship of pier

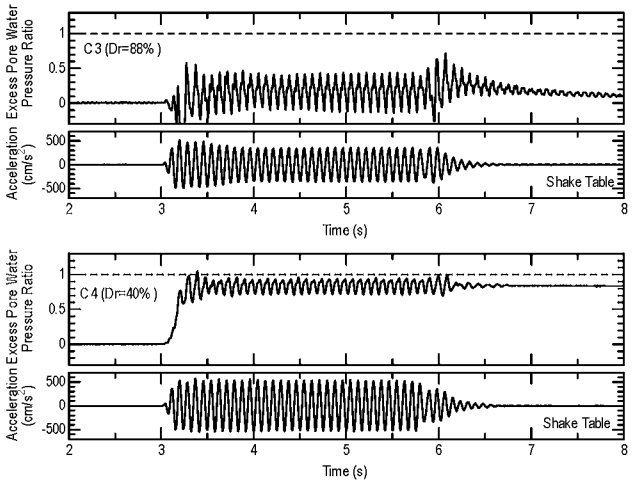


Figure 5 Excess pore water pressure ratio at 0.95m beneath the surface (Cases C3 and C4)

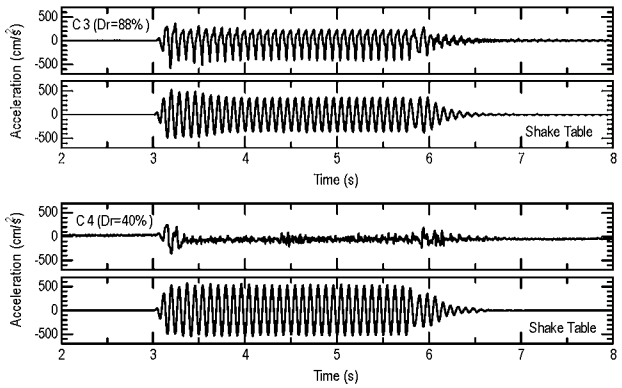


Figure 6 Acceleration at 0.95m beneath the surface (Cases C3 and C4)

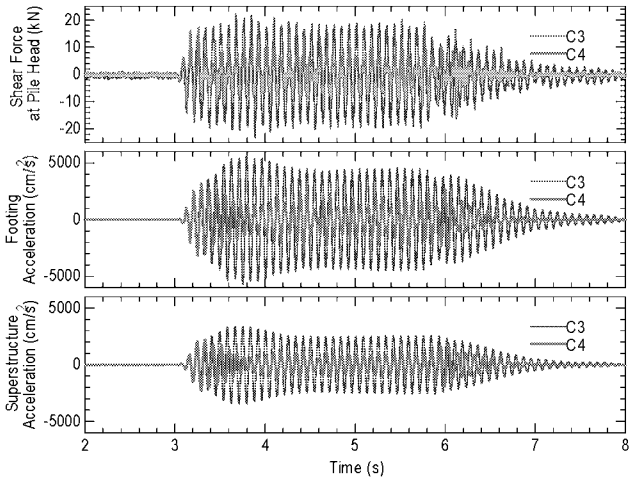


Figure 7 Shear force at pile head, accelerations at footing and superstructure (Cases C3 and C4)

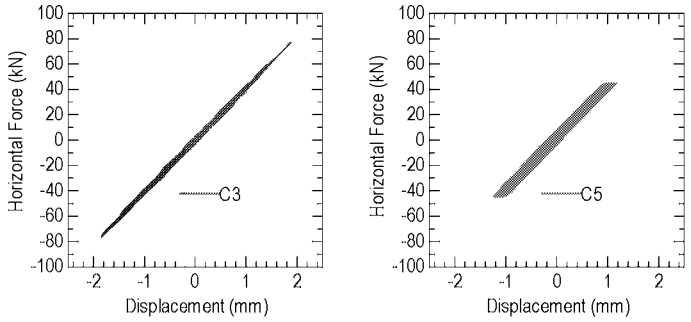


(a) Case C3 (b) Case C5

Figure 8 Horizontal force-displacement relationship of pier (Cases C3 and C5)

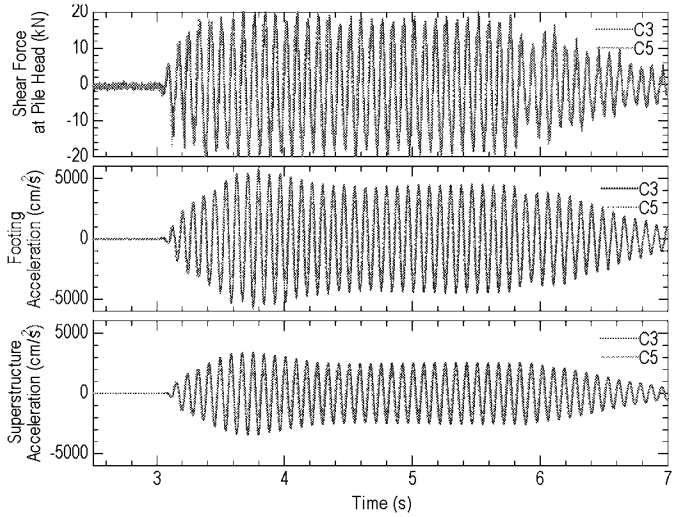


Figure 9 Shear force at pile head, accelerations at footing and superstructure (Cases C3 and C5)

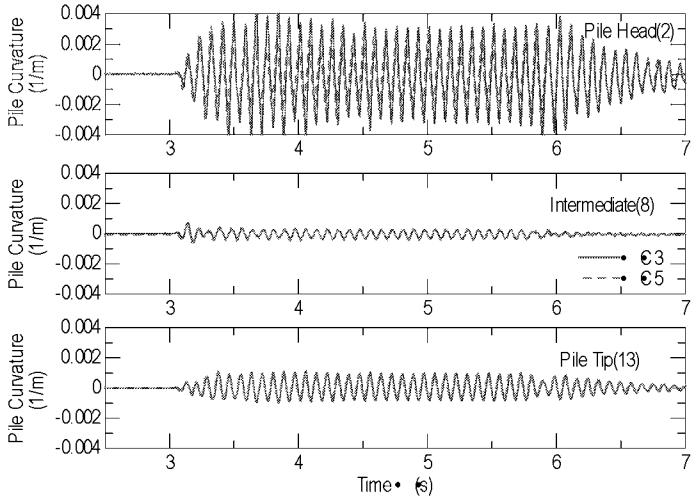


Figure 10 Pile curvature (Cases C3 and C5)

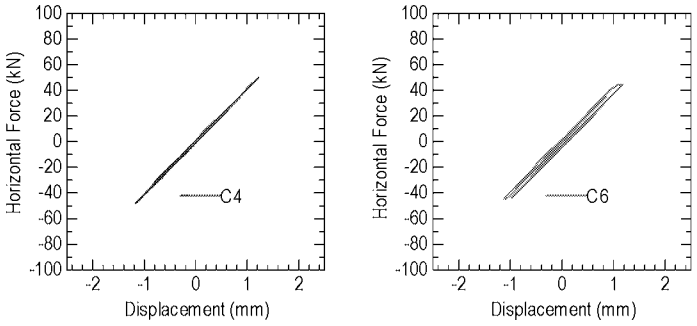


(a) Case C4 (b) Case C6

Figure 11 Horizontal force-displacement relationship of pier (Cases C4 and C6)

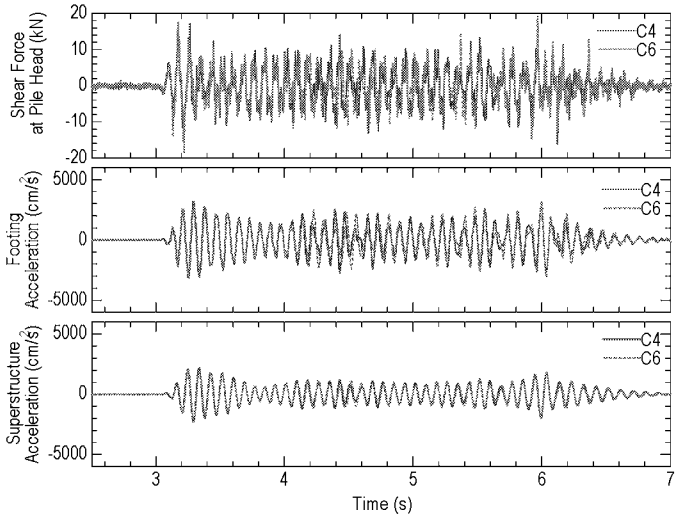


Figure 12 Shear force at pile head, accelerations at footing and superstructure (Cases C4 and C6)

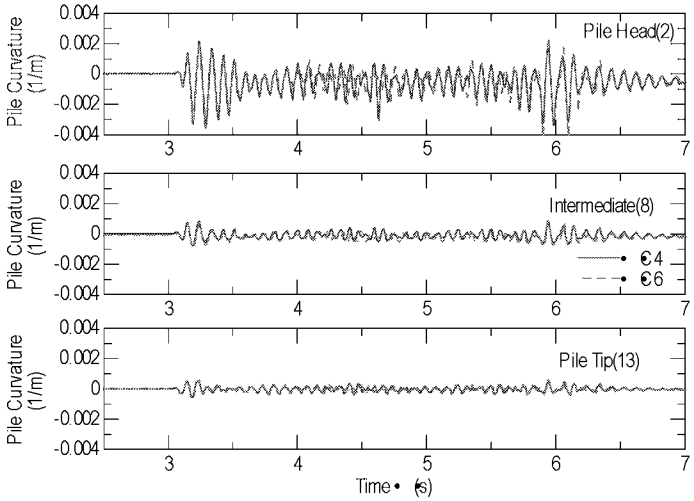


Figure 13 Pile curvature (Cases C4 and C6)

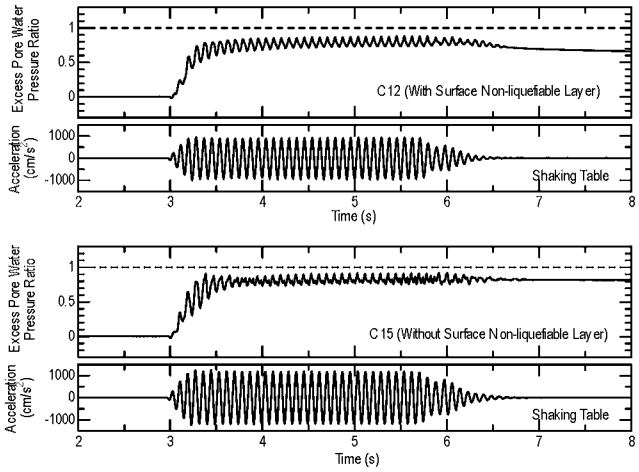


Figure 14 Excess pore water pressure ratio at 1.35m beneath the surface (Cases C12 and C15)

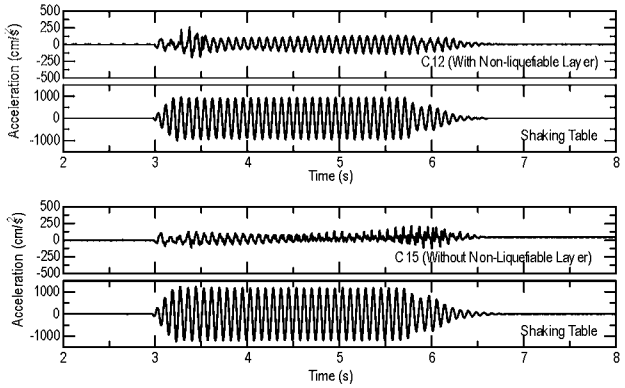


Figure 15 Acceleration at 1.35m beneath the surface (Cases C12 and C15)

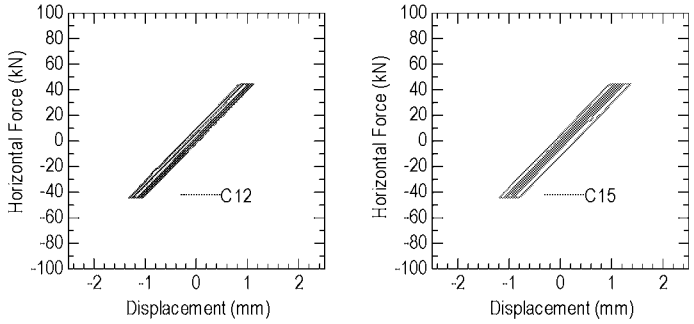


(a) Case C12 (b) Case C15

Figure 16 Horizontal force-displacement relationship of pier (Cases C12 and C15)

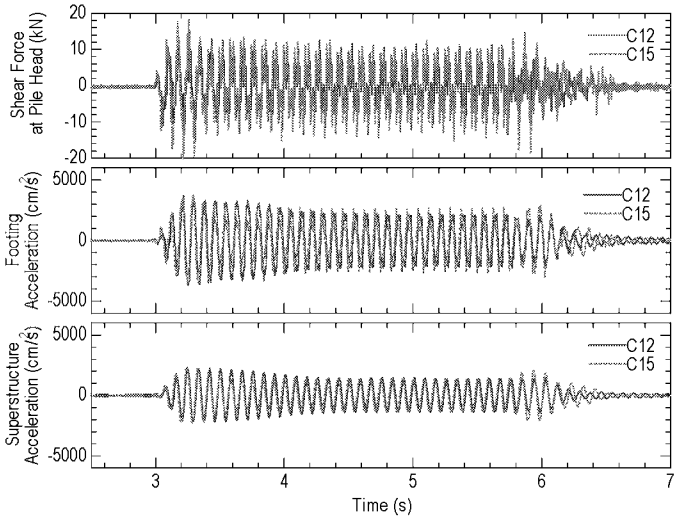


Figure 17 Shear force at pile head, accelerations at footing and superstructure (Cases C12 and C15)